ARTICLE IN PRESS

Available at www.ElsevierComputerScience.com
POWERED BY SCIENCE DIRECT®

PERGAMON

Pattern Recognition ▮▮▮ (▮▮▮) ▮▮▮–▮▮▮

PATTERN RECOGNITION
THE JOURNAL OF THE PATTERN RECOGNITION SOCIETY

www.elsevier.com/locate/patcog

Automated person recognition by walking and running via model-based approaches

ChewYean Yam, Mark S. Nixon*, John N. Carter

Department of Electronics and Computer Science, University of Southampton, Southampton SO17 1BJ, UK

Received 2 July 2002; received in revised form 1 August 2003; accepted 22 September 2003

Abstract

Gait enjoys advantages over other biometrics in that it can be perceived from a distance and is difficult to disguise. Current approaches are mostly statistical and concentrate on walking only. By analysing leg motion we show how we can recognise people not only by the walking gait, but also by the running gait. This is achieved by either of two new modelling approaches which employ coupled oscillators and the biomechanics of human locomotion as the underlying concepts. These models give a plausible method for data reduction by providing estimates of the inclination of the thigh and of the leg, from the image data. Both approaches derive a phase-weighted Fourier description gait signature by automated non-invasive means. One approach is completely automated whereas the other requires specification of a single parameter to distinguish between walking and running. Results show that both gaits are potential biometrics, with running being more potent. By its basis in evidence gathering, this new technique can tolerate noise and low resolution.

Keywords: Biometrics; Gait; Model-based; Coupled oscillator; Bilateral symmetry; Evidence gathering

1. Introduction

Identity theft is emergent and fast-growing, often involved in serious crime or even terrorist acts. As such, biometrics continue to gain increasing attention. Since biometrics concern using personal characteristics for identification, the possibility of identity fraud is significantly reduced. A biometric can be of any physiological or behavioural characteristic provided that it is universal, unique, permanent and collectable [1]. It is no surprise that airports show particular interest in biometric technology, given the attractive combination of high-speed processing, with a potentially high level of security. Other applications include the deployment of on-line face recognition and the use of fingerprints for access control.

Any biometric has its unique advantages and disadvantages, which often concern application and social issues. Fingerprint, iris and retinal pattern may enjoy uniqueness across large populations, but can be difficult to collect as they require a subject's co-operation. On the other hand, face, ear and signature data can easily be acquired, but may be concealed or disguised to avoid (remote) identification. Gait may have the potential to overcome these limitations. One of the unique advantages of using gait as a biometric is that it can be perceived from a distance, making acquisition non-invasive and convenient. Biometrics such as the iris and retinal patterns and face require high-resolution images whereas surveillance cameras are often of poor resolution. Gait will not suffer from this shortcoming because the body is proportionally larger area compared with the eyes or face. Further, it does not restrict viewpoint as much as other personal characteristics. As such, gait appears to be suited to addition to the current stock of biometrics. Furthermore, gait cannot be easily disguised without impeding one's natural walk (which could attract attention). Naturally, as gait is a behavioural biometric, it can be

* Corresponding author. Tel.: +44-2380-593542; fax: +44-2380-594498.
E-mail address: msn@ecs.soton.ac.uk (M.S. Nixon).

0031-3203/$30.00 © 2003 Pattern Recognition Society. Published by Elsevier Ltd. All rights reserved.
doi:10.1016/j.patcog.2003.09.012

affected by drunkenness, pregnancy, diseases, footwear and load.

There is considerable evidence in the literature that humans have a natural ability to recognise friends by their walk. Psychological studies confirmed that we can discriminate the gender of a walker [2]. Studies of human locomotion found that male walkers tend to swing their shoulders more while female walkers tend to swing their hips more [3]. Recently, the walking styles of children and adult have been categorised via computer vision techniques [4]. We can also recognise ourselves and acquaintances by a dynamic light display of the walking pattern [5] without familiarity cues. It is suggested that gait could be used as a reliable means for discrimination, especially when the face is obscured [6] because individuals show unique characteristics in their walking mechanics [7].

Human motion analysis has gained increasing attention from computer vision researchers motivated by a wide spectrum of applications such as surveillance, medical, man–machine interface and animation. The major areas of research are motion analysis [8,9], tracking [10,11], recognizing biological motion [12,13], and now as a biometric. Investigations into gait as a biometric only began about a decade ago. Perhaps the earliest work derived a gait signature from a spatio-temporal pattern of a walking person for recognition purposes [14]. Murase and Sakai [15] projected images of human walking in eigenspace and used the eigenvectors for gait recognition. Then, dense optical flow [16] was exploited where an instantaneous motion description that varies with the type of motion and the moving objects was developed. Huang [17] combined canonical space transformation based on Canonical Analysis with eigenspace transformation for feature extraction to extract a gait signature. More recently, the potential of image self-similarity [18], area-based metrics [19], static body parameters [20], velocity moments [21] and symmetry [22] have been used to generate gait signatures. Approaches discussed so far measure changes in a subject's silhouette. However, the significant information in, or characteristics of, a gait pattern is the interaction and inter-relationship of a structural description. Although there exist methods for modelling human motion, these have not been deployed for identification purposes. The only model-based approach in human gait recognition was pioneered by Cunado who explored the potential of the velocity hough transform (VHT) and a simple pendulum model [23]. This approach models human walking by representing the thigh as a pendulum. It combines the VHT with a Fourier series to describe the leg's motion within a gait cycle. The gait signature is then derived from the Fourier series. Visually, leg movements during walking and running resemble a compound pendulum, that is, the leg is periodically swinging at a fulcrum. Thus, adapting pendular motion to model human locomotion would appear appropriate. This idea has led biomechanicists to consider leg movements as free and forced oscillation [24].

Until now, much research has focused on human walking with encouraging results that confirm the potential of using walking gait as a biometric. Consequently, it is of interest whether recognition by running can offer equivalent capability, or even better, for identifying people. Although walking and running are distinct gaits as defined by biomechanics, interestingly, it has been demonstrated that there occur topological similarities in the co-ordination patterns between the thigh and the lower leg during walking and running [25]. Since walking and running are intimately related by the skeleto-muscular structure, it would appear reasonable to suggest that there exists some correlation between them. Given this inter-relationship, then it may suggest that there should exist a single model with capability to describe both gaits.

Accordingly, our objective here is to develop an automated non-invasive model-based approach to recognise people by walking and running. Our data is laboratory-based, aiming to analyse basic capabilities. Clearly, an application scenario will exacerbate problems with data acquisition and analysis. Our motivation here was to determine whether or not any putative link between running and walking could be exploited for recognition purposes. Should that link exist then practical development mandates use of treadmills for acquisition and in consequence further study of the effect of treadmills on gait, and the translation to real-world scenarios. But that is for later, rather than at this introductory stage. In order to extract leg motion, we need to know where the *moving legs* are. This makes essential the biomechanical basis of human locomotion outlined in Section 2. Section 3 describes the evidence gathering technique used to extract the leg motion. Borrowing the concept of pendulum motion to aid motion extraction, we have developed two new models, that both have capability to describe walking and running, as described in Section 4. These models are used to drive a feature extraction stage, which essentially maps moving lines in the image data. One model is empirical and the other is analytical, and the latter employs the concept of a forced coupled oscillator. Later we show how the analytical model can offer improved recognition performance compared with the empirical model, and with greater freedom in deployment. These models do not describe gait precisely, but guide a temporal evidence gathering technique. Phase-weighted Fourier description gait signatures are then derived from the extracted movement (Section 5). This technique has been evaluated on a database of 20 walking and running subjects and the results are discussed in Section 6. Section 7 draws conclusions and discusses the future direction of this approach.

2. Human gait

Gait is known as one of the most universal and yet most complex form of all human activities. It involves a high level of interaction between the central nervous system and

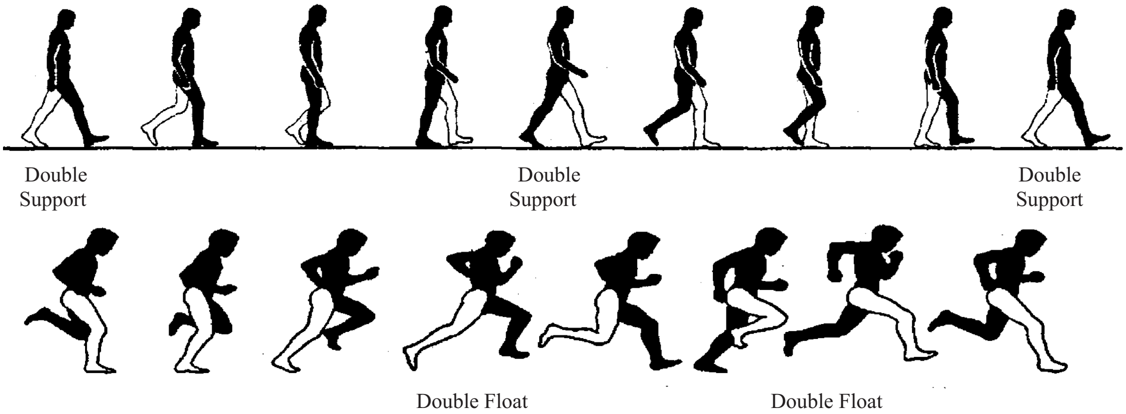

Fig. 1. Comparison of a gait cycle for walking and running.

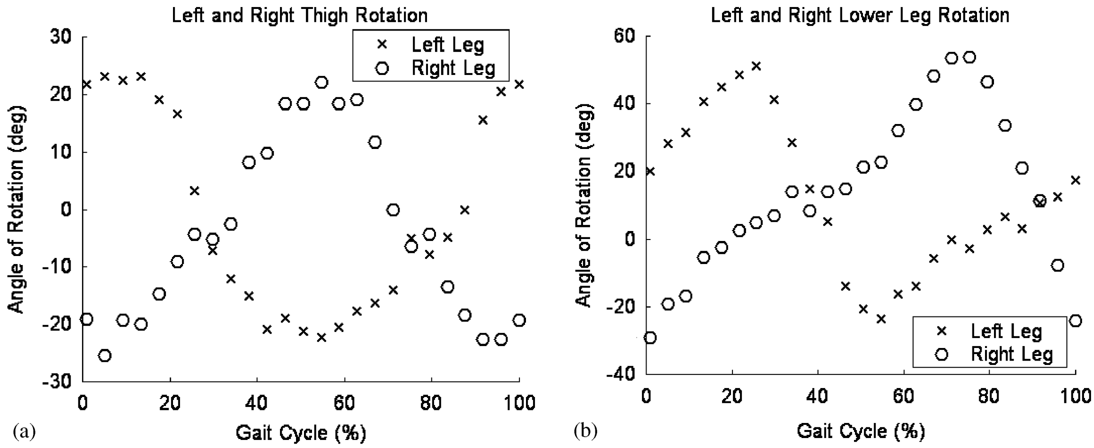

Fig. 2. Thigh and lower leg rotation of the left and right leg with half a period phase shift.

various muscles to allow an individual to keep the body upright, while moving around in an orderly and stable manner. Hence, understanding the underlying mechanism of walking and running is essential when developing an approach that is well suited to describe the motion for the purposes of acquiring data for biometric deployment. Although Aristotle was the first to study human gait [26], the normal walking gait pattern has been characterised and quantified [27] only recently. Running is a natural extension of walking, with significant biomechanical differences [28]. By a biomechanics definition, walking and running are distinguished first by the stride duration, stride length, velocities and the range of motion made by the limbs. The kinematics of running differ from those of walking where the joints' motion increases significantly as the velocity increases. The most distinctive difference concerns the existence of periods of *double support* or *double float*. For walking there exists a period where both feet are in contact with the ground (*double support*), whereas for running, there exists a period where both feet are not in contact with the ground (*double float*), i.e. airborne. This is illustrated in Fig. 1. Another difference is the manner in which the foot contacts the ground. During walking, the heel contacts the ground by a foot-flat stance. For running, the majority of runners are rear-foot or heel strikers while some are mid-foot strikers [29,30], increasing variability in running gait pattern.

2.1. Pattern of movement

Human locomotion is naturally rhythmic producing a co-ordinated oscillatory behaviour [31] which is believed to be controlled by the central pattern generator. One of the unique characteristics of walking and running is bilateral symmetry, that is, when one walks or runs, the left arm and right leg interchange direction of swing with the right arm and left leg, and vice versa, with a phase shift of half a period. Fig. 2 shows the manually labelled absolute angle of rotation for thigh and lower leg of both legs with respect to the vertical. This shows that the motions of the left and right leg are coupled by half a period phase shift. However, this is only a generalisation for normal gait. Gait symmetry or asymmetry has been a constant topic of discussion among the biomechanics community [32]. As our purpose here is to develop a model to guide the system in extracting leg motion, gait symmetry can be assumed. Hence, the same model can describe either leg since both perform the same motion but out of phase with each other by half a period. These motions operate in space and time, satisfying the rules of spatial symmetry (sequence of oscillation, i.e. swapping legs and arms) and temporal symmetry (a phase-lock of half a period in general). Both legs can be modelled by two distinct but systematically coupled oscillators, which oscillate at the same frequency (frequency-lock) but with fixed relative phase difference.

3. Gait modelling and analysis

In order to extract the motion of the thigh and lower leg, we first have to acquire the motion of the hip, then the thigh and finally the lower leg. This section illustrates the model of the hip motion, the bilateral symmetric and the forced coupled oscillator model describing the thigh and lower leg motion, which will assist in locating and extracting the moving leg and the motion simultaneously. These models will enable selection, from images, of data pertaining to the motion of the front of the leg(s). This ensures that we use human movement data, rather than the model, for recognition. This is in direct contrast with the only other model-based approach [23] that accumulated a Fourier-based gait signature direct from the edge data and had no guiding process as to the edge data selected.

3.1. The hip motion model

Treadmills offer many advantages in the collection of data for analysing human locomotion such as space requirements are constrained, environmental factors can be controlled, steady-state locomotion speeds are selectable, and successive repetitive strides can be documented. Whether a treadmill will change the pattern of walking and running has been debated much in the biomechanical, physiological and rehabilitation literature. One experimental study suggests that walking on an 'ideal' treadmill does not differ mechanically from walking over ground, except for wind resistance, which is negligible during walking [24]. The only difference between the two conditions is perceptual: during walking, the environment is stationary [33]. On the other hand, some studies have found statistically significant differences in the displacements of the head, hip and ankle. However, in general, treadmill walking was not found to differ markedly from floor walking in kinematics measurements [34]. Whether treadmills affect one's gait will also depend on the habituation of the subjects to treadmill walking [35]. For this reason, all the subjects here were familiarised to the treadmill before filming. However, for our purposes we assume all subjects to be affected equally as they were all filmed under the same conditions. Thus, the features may change, but with respect to one another, these changes are assumed to be insignificant.

Subjects were filmed walking and running on a motorised treadmill at constant velocities. Because the horizontal position of the hip is known and the resolution of the images used is relatively low, the horizontal motion of the hip is insignificant compared with the other motions, such as the hip's vertical oscillation and the motion of the thigh and lower leg. The vertical motion of the hip is essential as it differs from walking to running. As depicted in Fig. 3, during running the amplitude of the displacement is greater and has a relative phase shift with respect to that of walking. The underlying model for the hip's vertical displacement, S_y, is

$$S_y(t) = A_y \sin(2\omega_y t + \phi_y), \tag{1}$$

where A_y is the amplitude of the vertical oscillation, ω_y is the fundamental frequency, ϕ_y is the phase shift and t is the time index for the normalised gait cycle. Here, all the plots are normalised to a complete gait cycle so that they are invariant to speed. Since a gait cycle consists of two steps, the frequency is twice that of the thigh motion, which will be described later. That is, every time we make a step, the body lowers and lifts, which gives the variations as shown in Fig. 3. The superimposed graphs reflect the veracity of this simple model, by comparing the model generated vertical rotation of the hip with that of manually labelled data. The structure is clearly similar and agrees with biomechanical studies acquired by marker-based systems [27,29].

3.2. The thigh and lower leg motion model

3.2.1. Bilateral symmetric model

This model is developed based on observation of the apparent movement of the human leg. The leg can be modelled as two penduli joined in series, as illustrated in Fig. 4. Following the biomechanics convention, the angle of knee rotation of this model is relative to the thigh rotation. The thigh rotation, $\theta_T(t)$, is described by Eq. (2), where A_T is the amplitude of the thigh rotation, ω_T is the frequency, ϕ_T is the phase shift and C_T is the offset.

$$\theta_T(t) = A_T \cos(\omega_T t + \phi_T) + C_T. \tag{2}$$

Eq. (2) can be applied for both running and walking. Figs. 5a and b show an example model-generated thigh rotation superimposed on the manually labelled data of a walking and running subject, respectively. The match

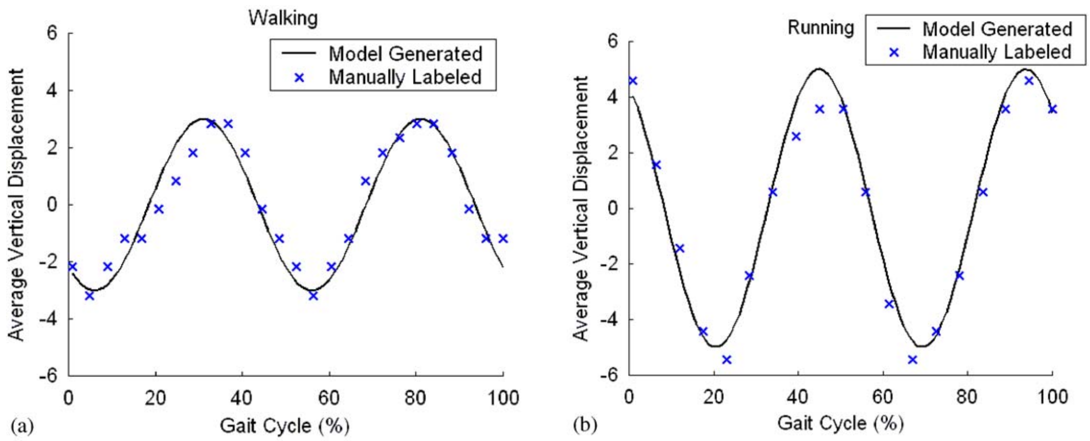

Fig. 3. The relative vertical displacement of hip during walking and running.

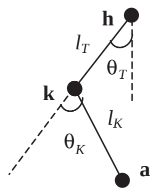

Fig. 4. The model of the thigh and lower leg: upper and lower pendulum models the thigh and the lower leg, respectively; connected at the knee joint.

appears reasonable, given the potential for error in manual labelling, and is well within the variance limits specified in medical studies [27]. The knee rotation, $\theta_K(t)$, can be described as

$$\theta_K(t) = \begin{cases} A_{K1}\sin^2(\omega_{K1}t) + C_k & 0 \leqslant t < p, \\ A_{K1}\sin^2(\omega_{K1}t + \phi_K) + C_k & p \leqslant t < 1, \end{cases} \tag{3}$$

where A_{K1} and A_{K2} are the amplitudes of the knee rotation, ω_{K1} and ω_{K2} are the frequencies, C_K is the offset, ϕ_K is the phase shift and p is the time when the second *double support* (walking) starts and the *double float* (running) starts. Observations show that p appears to be approximately 0.4 for walking and 0.3 for running. This is because the swing phase starts earlier in running. An example result shows that the $\sin^2$ term models the basic motion well, as depicted in Fig. 5(c) and (d). Here, the broad shape matches well, so the model does indeed appear to be an appropriate basis for development. As such, a model which has fewer parameters as compared to the earlier model [36] and able to describe both walking and running gait, coupling the left and right leg by a phase-lock of half a period shift, has been developed. Again, they agree with biomechanical observations [27,29].

3.2.2. *Forced coupled oscillator model*

Although the bilateral symmetric model illustrated earlier offers a good representation for the motion, there are several drawbacks. First of all, the model lacks analytical attributes, and secondly there is a need to select the gait mode, i.e., a value for the parameter p. In our new model the human lower limb is again represented by two penduli joined in series, but $\theta_K(t)$ is measured with respect to vertical (the absolute angle) as opposed to the one in the bilateral symmetry model which is relative to $\theta_T(t)$, see Fig. 6. We exploit the concept of a forced coupled oscillator in creating a model invariant to walking and running gait, as legs were considered to be imperfect penduli with substantial energy loss [24]. Studies in biomechanics have shown that a driven harmonic oscillator provides a good representation for human walking [37]. However, this is usually a simple pendulum representing the thigh motion only. Our new model solves the differential equations obtained from the dynamic model of the coupled penduli and describes the motion of the thigh and the lower leg, simultaneously. To avoid notational overload, the corresponding labels remain the same for this new model, as for the previous one in Section 3.2.1.

Referring to Fig. 6, let us consider the upper pendulum modelled by simple harmonic motion as

$$\ddot{\theta}_T + \omega_T^2\theta_T = 0, \tag{4}$$

where θ_T is the angular displacement from the vertical, $\ddot{\theta}_T$ is the angular acceleration, and ω_T is the natural frequency. The solution is the basic motion model for thigh rotation,

$$\theta_T = A\cos(\omega_T t) + B\sin(\omega_T t), \tag{5}$$

where A and B are constants, and t is a time index which varies from 0 to 1, representing the start and end of the gait cycle, respectively.

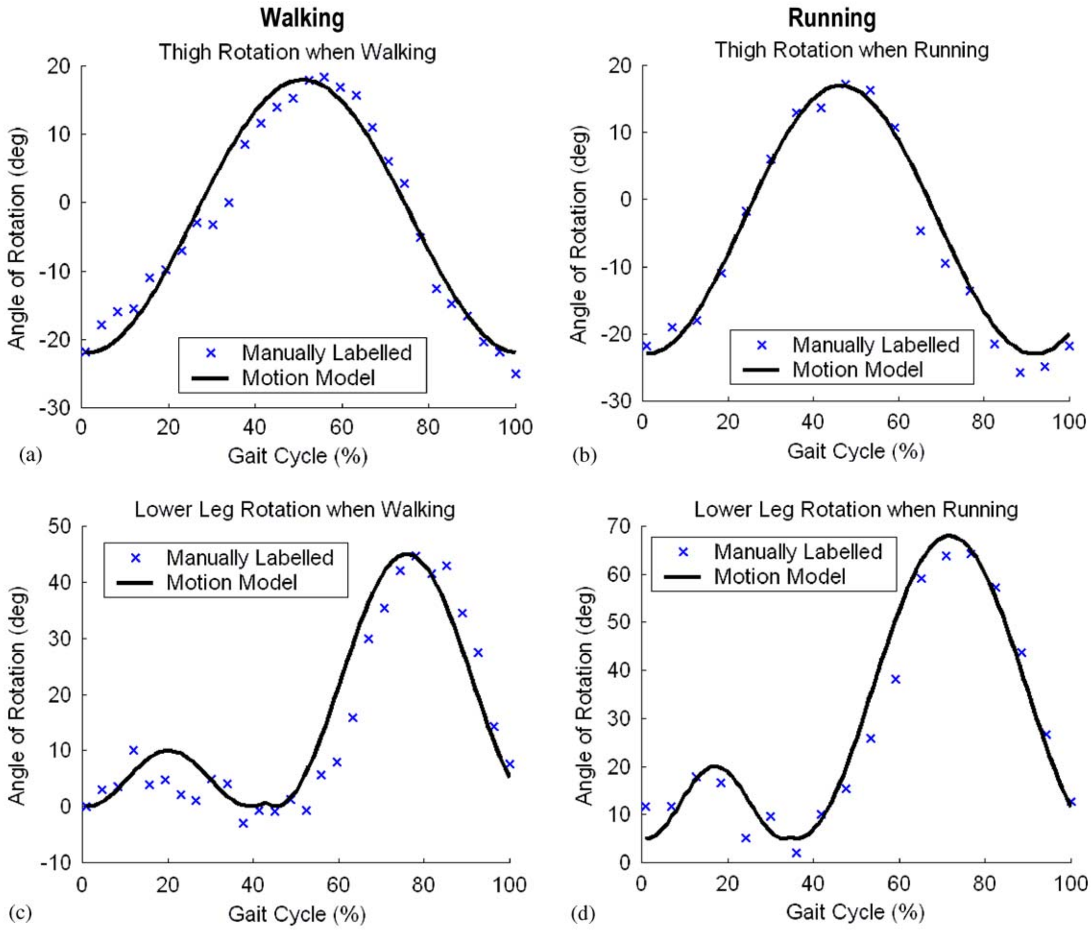

Fig. 5. The model-generated and manually-labelled thigh and knee rotation for walking and running.

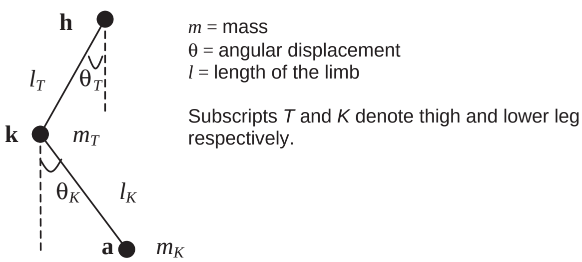

Fig. 6. The dynamically coupled pendulum model.

In reality, human walking and running is a highly sophisticated system involving multiple factors interacting simultaneously. Naturally, realistic modelling of an individual's locomotion is unnecessary as we seek only the basic structure to guide the motion extraction process. Identity is then associated with consistent pattern of difference from the individual basic structure. We shall assume that the lower leg can be modelled as a driven oscillator where the force applied to it is related to the motion of the upper pendulum. Following an analogy of Newton's laws, by differentiating Eq. (5) twice, we have

$$\ddot{\theta}_T = -\omega_T^2[A\cos(\omega_T t) + B\sin(\omega_T t)] \tag{6}$$

which contributes to the driving force to the lower pendulum. This force is given by

$$\mathbf{F}(t) = -m_T\omega_T^2[A\cos(\omega_T t) + B\sin(\omega_T t)]. \tag{7}$$

Similar to Eq. (4), the motion equation for the lower pendulum is

$$\ddot{\theta}_K + \omega_K^2\theta_K = -\mathbf{F}(t). \tag{8}$$

Substituting Eq. (6) into Eq. (8), yields

$$\ddot{\theta}_K + \omega_K^2\theta_K = m_T\omega_T^2[A\cos(\omega_T t) + B\sin(\omega_T t)]. \tag{9}$$

The solution for θ_K will comprise the general solution, θ_{Kg}, and the particular solution, θ_{Kp}. The general solution is obtained by setting $\mathbf{F}(t) = 0$ in Eq. (8) to give

$$\theta_{Kg} = C\cos(\omega_K t) + D\sin(\omega_K t), \tag{10}$$

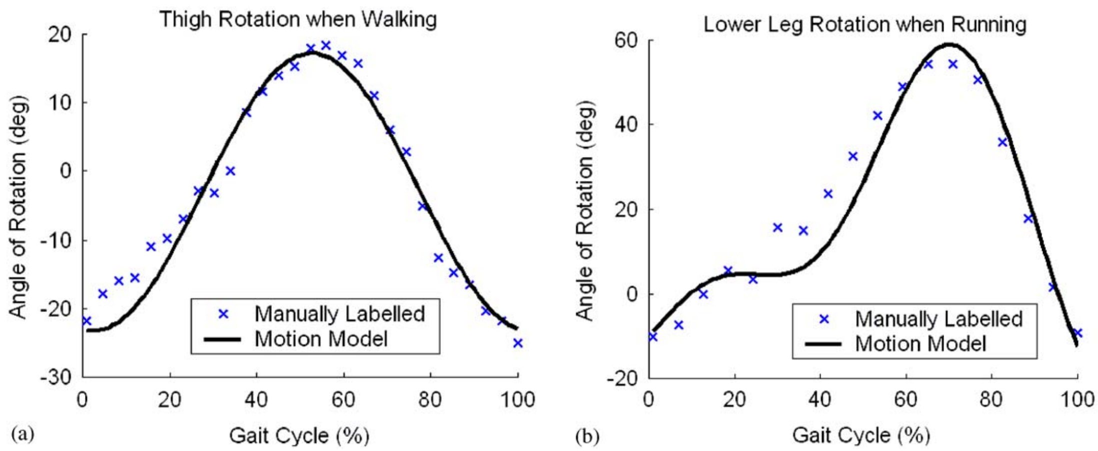

Fig. 7. Sample output of the thigh and lower leg motion model superimposed on manually labelled data.

where C and D are constants. A Wronksian method is used to find the particular solution, and the result is

$$\theta_{Kp} = -\frac{m_T\omega_T^2}{(\omega_T^2 - \omega_K^2)}(A\cos\omega_T t + B\sin\omega_T t). \quad (11)$$

Recalling that $\theta_K = \theta_{Kg} + \theta_{Kp}$, by substituting Eqs. (10) and (11), the complete solution for θ_K yields the basic motion model for the lower leg rotation, which is

$$\theta_K = C\cos\omega_K t + D\sin\omega_K t - \frac{m_T\omega_T^2}{(\omega_T^2 - \omega_K^2)}(A\cos\omega_T t + B\sin\omega_T t). \quad (12)$$

These motion models are not sufficient to guarantee a good approximation in implementation since we do not walk or run like a pendulum. If we did, we would not move at all! One obvious reason is that our legs do not swing about an equilibrium point. We approximate by pendular motion only to guide an automated motion extraction process.

An example waveform produced by the thigh and lower leg motion models is shown in Fig. 7. The structure of the response of the model appears close to that of the manually labelled data (as can be seen $\omega_K \simeq 1.96\omega_T$, nearly twice its value as expected). As expected the simple model does not match the rotation precisely, but can describe the gross motion of the lower leg, over a single gait cycle. It is periodic over a larger time interval but not within the gait cycle itself. In fact, the model can be viewed to select the portion, of a much longer signal, that matches the known shape of gait data, and is justifiable in its derivation. As we shall see, it serves as a model to automatically extract gait motion for one cycle via computer vision techniques. It is more likely that a better model of gait itself, employing Fourier descriptors could afford better characteristic capability but at the expense of complexity. The results here suggest such an approach is unnecessary.

3.3. Structural model of thigh and lower leg

Referring to Fig. 6, the structure of the thigh in both models can be described by a point **h** that represents the hip and the line passing through **h** at an angle θ_T. The knee is then

$$\mathbf{k}(t) = \mathbf{h}(t) + l_T\mathbf{u}_T(t), \quad (13)$$

where $\mathbf{u}_T(t)$ is the unit vector of the line direction, **h** is the position of the hip and l_T is the thigh length, as $\mathbf{u}_T(t) = [-\sin\theta_T(t), \cos\theta_T(t)]$ and $\mathbf{h}(t) = [h_x(0), h_y(0) + S_y(t)]$, where $h_x(0)$ and $h_y(0)$ are the initial hip coordinates. Decomposing Eq. (13) into constituent parts yields the coordinates of the knee point as,

$$k_x(t) = h_x(0) - l_T\sin\theta_T(t), \quad (14)$$

$$k_y(t) = h_y(0) + S_y(t) + l_T\cos\theta_T(t). \quad (15)$$

Similarly, the structure of the lower leg is given by a line which starts at the knee, that passes through **k** at an angle θ_k. The ankle **a** is

$$\mathbf{a}(t) = \mathbf{k}(t) + l_K\mathbf{u}_K(t), \quad (16)$$

where $\mathbf{u}_K(t)$ is the unit vector of the line direction, $\mathbf{k}(t)$ is the position of the knee and l_K is the lower leg length, as $\mathbf{u}_K(t) = [-\sin(\theta_K(t)), \cos(\theta_K(t))]$ and $\mathbf{k}(t) = [k_x, k_y]$, where k_x and k_y is the point of knee. Decomposing Eq. (16) into constituent parts yields the coordinates of the ankle as

$$a_x(t) = k_x(t) - l_K\sin(\theta_K(t)), \quad (17)$$

$$a_y(t) = k_y(t) + l_K\cos(\theta_K(t)). \quad (18)$$

Hence, the motion models for walking and running coupling the thigh and the lower leg and the structural model have been derived. These form the basis of the template to

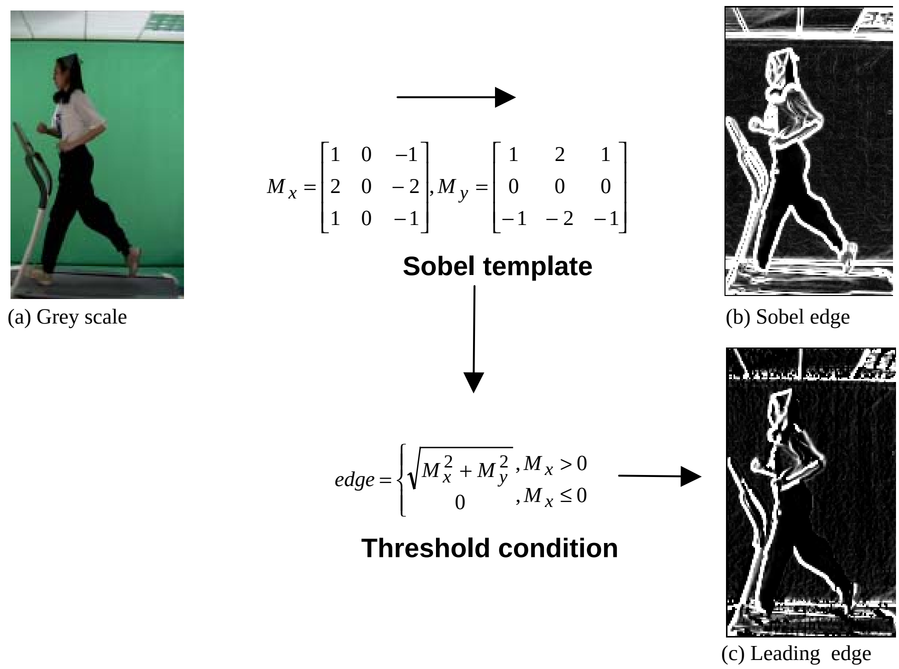

Fig. 8. Leading-edge detection.

be used within feature extraction to find the moving lines that correspond to a subject's leg.

4. Feature extraction

4.1. Low level

The subjects are filmed as video clips which are then digitised into individual colour image files and cropped to reduce computational cost. This primary evaluation concerns laboratory data. Later we shall seek to apply the new technique to outdoor data where there are more moving objects, as well as lighting variation. Certainly, it is likely that in real-world imagery there will be less contrast between the leg and its background than is experienced here. However, rather than develop a generalised application, we sought to first demonstrate that the new approach could indeed operate with success on laboratory-derived data. To further reduce the complexity of the colour image, the Sobel edge operator is applied to the three colour planes (red, green, blue). A condition, which effectively thresholds the x-component of the Sobel edge operator, is applied to obtain only the leading edge of a subject whose clothing is darker than the background. The leading edge is most suited to automate extraction because clothing adheres most to the front of the moving leg. The edge data of three layers are then added and thresholded, to produce prominent edges. Fig. 8 shows the templates used to extract (b) the edge data and the condition applied to extract only (c) the leading edge.

4.2. Evidence gathering by temporal template matching

The evidence gathering technique used here comprises two stages: (i) global/temporal template matching across the whole sequence and, (ii) local template matching in each image. The aim of the first stage is to search for the best motion model that can describe the leg motion well over a gait cycle, i.e. the gross motion of a complete gait cycle. This is essentially trying to match a line which moves according either to the structural or to the motion model described in Section 3, to the edge maps of a whole sequence of images to find the desired moving object. This gives estimates of the inclination of the thigh and of the lower leg which are refined by a local matching stage in each separate image. As such, we first capture the general motion and then refine it aiming to ensure that we have captured local variation from the global solution. The whole process is illustrated in Fig. 9.

In the first stage, essentially we seek values for the parameters that maximise the match of the moving line to the edge data, evaluated across the whole sequence, as those parameters

$$A_i, B, C, D, \omega_K, \omega_T = \max\left(\sum_{t \in r} \sum_{x \in image} \sum_{y \in image} (P_{x,y}(t) = MT_{x,y}(t)) \right), \qquad (19)$$

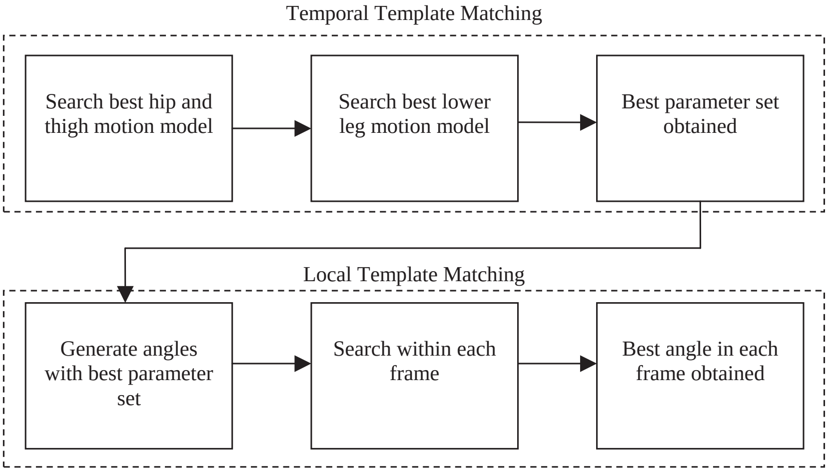

Fig. 9. Extracting the motion of lower limb.

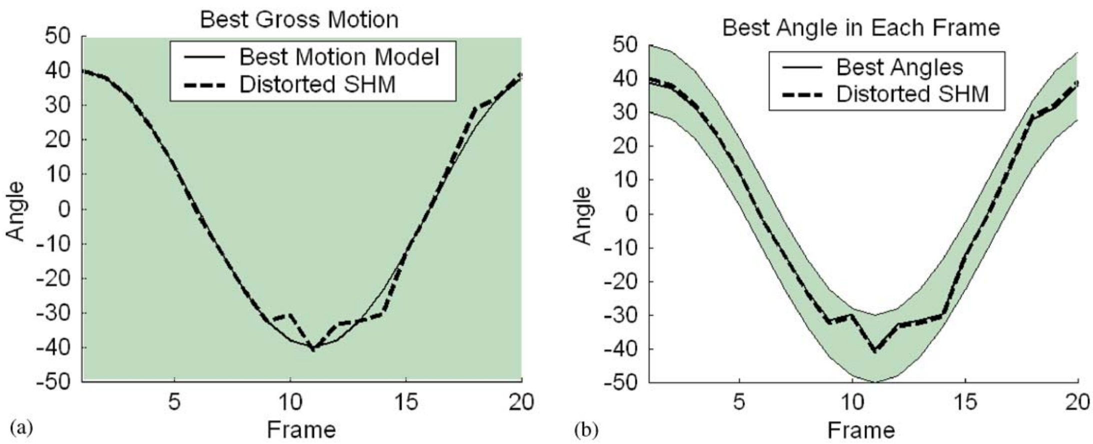

Fig. 10. Results of (a) temporal template matching and (b) local template matching, where shaded area is the search space.

where P is the image and MT is the motion template (with dynamics derived from either the structural model of Eqs. (2) and (3) or the motion model of Eqs. (5) and (12). Having found the best set of parameters, the estimated thigh and lower leg inclination for each frame are then generated. These angles form the basis of a local search for the best fit line to the data in each single image, as

$$\theta_K, \theta_T = \max\left(\sum_{x\in image}\sum_{y\in image}(P_{x,y} = AT_{x,y})\right), \tag{20}$$

where AT is the line resulting from application of the motion template, with variation of up to $\pm 5^\circ$ in inclination and ± 5 pixels in vertical and horizontal translation. This will ensure that the best-fit angle and position is found in each frame.

Fig. 10 illustrates the process of extracting a simulated moving lower limb employing this evidence gathering technique. The simulation is based on SHM to which some noise has been added. This results in the motion represented by the dotted lines in Fig. 10. Initially, Fig. 10(a), the whole space is searched (as indicated by the shading) by the motion model resulting in an estimate represented by the solid line in Fig. 10(a). This estimate (with variation here of $\pm 10^\circ$, twice that used in actual gait studies in view of the range of motion here) primes the local feature match process with the shaded range shown in Fig. 10(b). Search within this range results in an extraction that matches the target data—the solid line that matches the dotted line in Fig. 10(b).

As depicted in Fig. 11, the result of this technique using the forced coupled oscillator model appears to extract well the thigh and lower leg motion without the need of

(a) Running (b) Walking

Fig. 11. Leg motion extraction results of running and walking by temporal template matching.

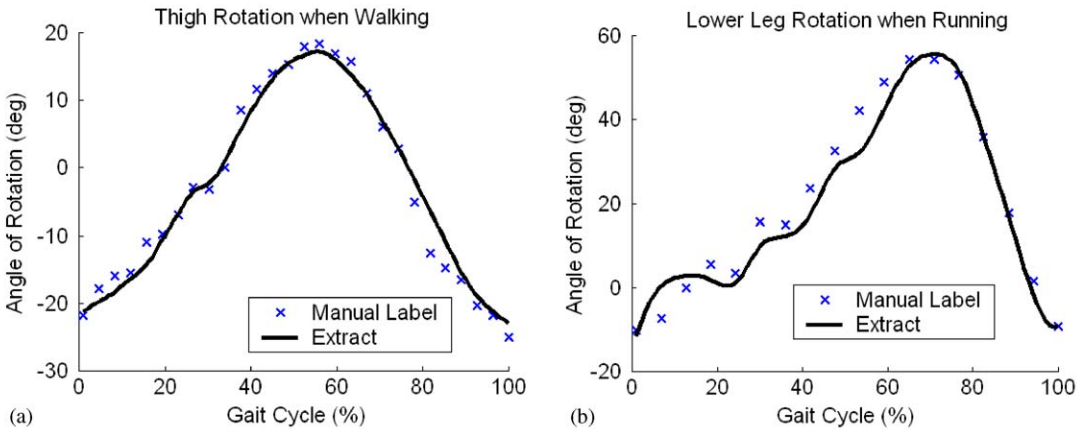

Fig. 12. Automatically extracted results superimposed with manually labelled data.

parameter selection, despite the fact that walking and running are two different gaits. The extraction angles are precise in the regions where the legs cross and occlude each other. Fig. 12 shows the manually labelled data superimposed on the result of this evidence gathering technique with the forced coupled oscillator model as the underlying template. Here we can observe the difference in result obtained by local matching guided by a model, compared with the result of the model alone (Fig. 7).

5. Gait signature

The gait signature of a particular subject consists of the phase and the magnitude components of the Fourier description of the thigh and lower leg rotation measured from a gait cycle. Here, the significant features of periodic motion are captured. As a shift in the time domain will affect the phase in the frequency domain, the time domain signals are aligned to start at the same point, which is the minimum of the thigh rotation and the corresponding instance of time of the lower leg rotation. This ensures the validity of the inclusion of the phase components when creating the gait signature for comparison. By using data between two successive minima, recognition becomes invariant to speed as data within a complete gait cycle is used.

Statistical analysis is necessary to establish the basis of determining which features to use in creating a useful gait signature for discrimination purposes. This will in turn increase the correct classification rate (CCR). A statistical measure that describes the distribution of subjects, or class, clusters in the feature space is employed. The separation, $\mathbf{S}$, between the class means, normalised with respect to class covariances, is used. The separation, $\mathbf{S}_{i,j}$, between subjects i and j is given by a form of Bhattacharyya distance as

$$\mathbf{S}_{i,j} = [\mathbf{m}_i - \mathbf{m}_j]\left[\frac{\Sigma_i + \Sigma_j}{2}\right]^{-1}[\mathbf{m}_i - \mathbf{m}_j]^{\mathrm{T}}, \tag{21}$$

where $\mathbf{m}_i$ is the mean and Σ_i is the covariance of class i. The mean signature $\mathbf{m}_i$ for each class i is given by

$$\mathbf{m}_{i,k} = \frac{1}{M}\sum_{l=0}^{M-1} \mathbf{x}^i_{l,k}, \qquad k = 1, 2, \ldots, N, \tag{22}$$

where M is the number of experiments for class i, N is the number of Fourier harmonics used and $\mathbf{x}^i$ is an $M \times N$ data matrix of signatures for class i. The covariance matrix, Σ_i, is

$$\Sigma_i = \frac{1}{M}\sum_{l=0}^{M-1} (\mathbf{x}^i_l - \mathbf{m}_i)^{\mathrm{T}}(\mathbf{x}^i_l - \mathbf{m}_i). \tag{23}$$

Table 1
Values of $\bar{S}$ and σ^2 using different features: magnitude alone, PWM and PWM with higher orders

	Walking		Running	
	$\bar{S}$	σ^2	$\bar{S}$	σ^2
Magnitude	0.0623	0.0086	0.0512	0.0064
PWM	0.1506	0.0264	0.1710	0.0175
PWM higher order	0.0151	0.0052	0.0140	0.0072

Discriminatory capability can be deduced from the cluster separation measurement, $\mathbf{S}_{i,j}$. If this value is large, either the clusters are well separated or have low variance. Conversely, poor discriminatory capability derives from clusters which are closely spaced or with high covariance. Table 1 summarises the mean separation ($\bar{S}$), evaluated for all values in $\mathbf{S}$ except the diagonal, for signatures including: using the magnitude component only; the lower order phase-weighted magnitude; and including higher order phase-weighted magnitude of the Fourier description, which will be described later. The value of $\bar{S}$ is directly proportional to the overall discriminatory capability of a set of features. This is aided by analysis of the (sample) variance of the separation, again evaluated from $\mathbf{S}$ over all values except the diagonal. Fig. 13 shows values of $\mathbf{S}$ as an image for 20 subjects. The brighter the square, the higher the separation, hence better discriminatory capability.

Although the magnitude spectra of lower harmonics (i.e. the first two harmonics from thigh rotation and first three harmonics from lower leg rotation) show some discriminatory capability, gait is not only characterised by the range of motion, but also involves the central pattern generator and musculature that together control the way the limbs move. That is, walking and running are not only distinguished by their kinematics (the range of motion made), but also significantly related by their kinetics (the forces that cause the movement). This implies that it is not just the extent of motion, but also the timing. Hence, the magnitude components are multiplied by their respective phase components, to yield the phase-weighted magnitude (PWM) signature $\mathbf{x}$ for sequence l of subject i as

$$\mathbf{x}^i_{l,k} = |\Theta(\mathrm{e}^{\mathrm{j}\omega_k})| \bullet \arg(\Theta(\mathrm{e}^{\mathrm{j}\omega_k})), \quad k = 1, 2, \ldots, N, \tag{24}$$

where $\Theta(\mathrm{e}^{\mathrm{j}\omega_k})$ is the kth Discrete Fourier Transform component of the angular data, and $\bullet$ denotes the multiplication of each element in the vector, thus increasing discriminatory capability. The zero-order term is ignored to eliminate the effect of any offsets, so the gait signature contains only the features of the pure motion of a gait cycle. Letting $\arg(\Theta(\mathrm{e}^{\mathrm{j}\omega_k}))$ range from $-\pi$ to π will introduce discontinuity at point $\pm\pi$, that is, even though they are the same point, but they appear to be 'numerically' far apart in the feature or signature space. This will cause a negative effect on the classification process. To eliminate this, the phase is represented in the complex form to ensure continuity and also the one-to-one mapping. This ensures validity in implementation.

The inter-class separation is increased when low-order PWMs ($N_T = 2$ and $N_K = 3$) are used to form the gait signature. Overall discriminatory capability has also increased as the values of $\bar{S}$ increase significantly compared to those of the signature vectors comprised of the magnitude component only, see Table 1 which also shows the inter-class separation when higher orders (i.e. the first ten harmonics:

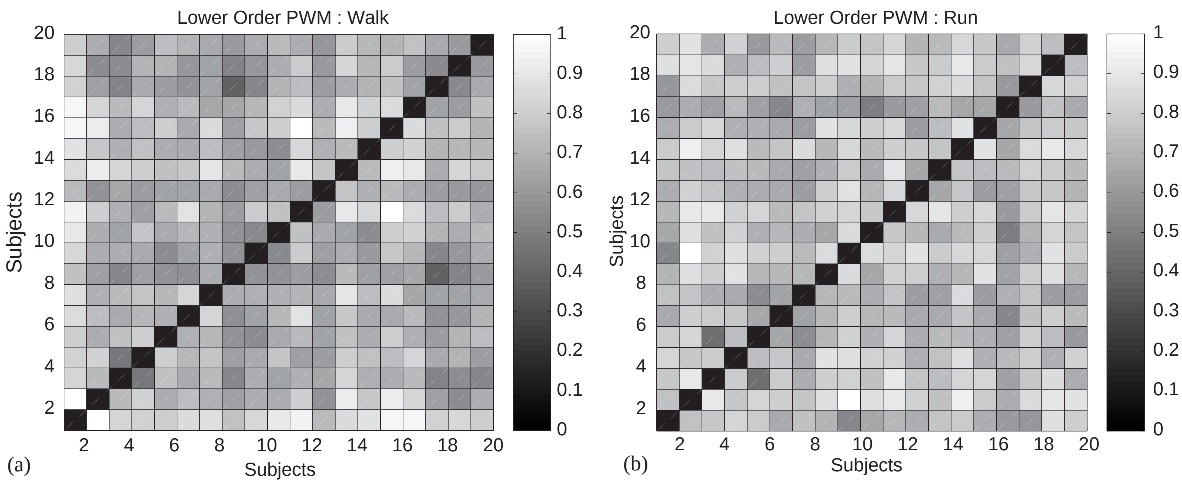

Fig. 13. Cluster separation of various feature vectors.

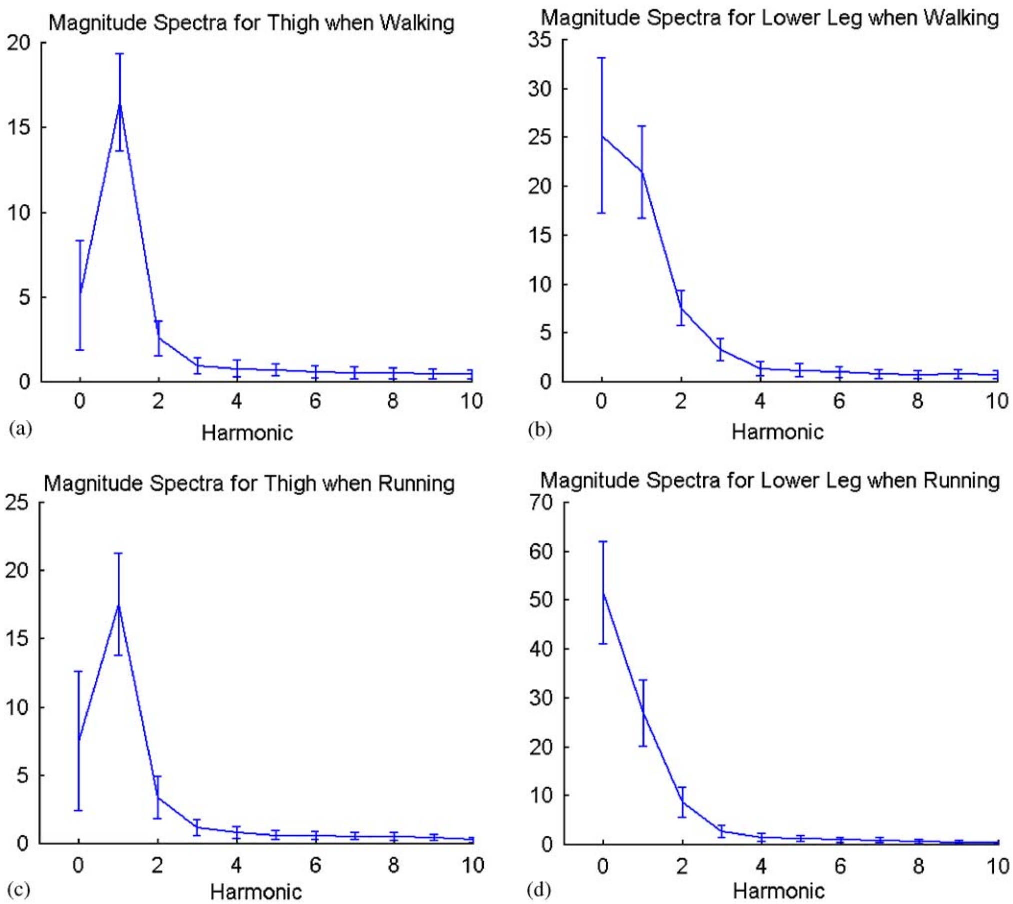

Fig. 14. Magnitude spectrum of thigh and lower leg rotation when walking and running, with standard deviation.

$N_T = 10$ and $N_K = 10$) are included in the signature vector. The values of $\bar{S}$ decreased compared with the signature vector using low order PWMs. This is because the PWMs of the thigh and lower leg rotation are dominated by the lower order components due to their greater magnitude, as shown in Fig. 14, where the error bar indicates the standard deviation computed from a population of 20 subjects, each with 5 samples. The magnitude of the higher order harmonics is relatively small and they are more likely to be dominated by noise. These are confirmed by the (sample) variance which is comparatively larger for the higher order components. This is supported by a medical study which suggested that the maximum frequency content of human walking is 5 Hz [38], that is, only the first five harmonics are sufficient to describe human locomotion.

6. Performance analysis

The database consists of 20 subjects walking and running on a treadmill at their preferred speeds with their own choice of clothing. There are 5 samples of walking and running for each subject. This database has more subjects than previous studies in gait recognition and is the first to contain the *same* subjects walking and running. The features are extracted via the evidence gathering technique described earlier, with the motion models as the underlying template. Performance analyses are carried out on both the bilateral symmetric and the forced coupled oscillator model and their results are discussed in the following subsections.

6.1. Result of bilateral symmetric and forced coupled oscillator model

Fig. 15 shows the signature formed from the thigh and lower leg rotation using the forced coupled oscillator model. For visualisation purposes, only 3 of the PWM components of 4 subjects are shown. Different symbols represent different subjects, each subject with 5 samples of walking and running. As depicted, there are well-defined intra-class boundaries for both gaits. Running appears to have greater inter-class variability, as confirmed by the decrease in

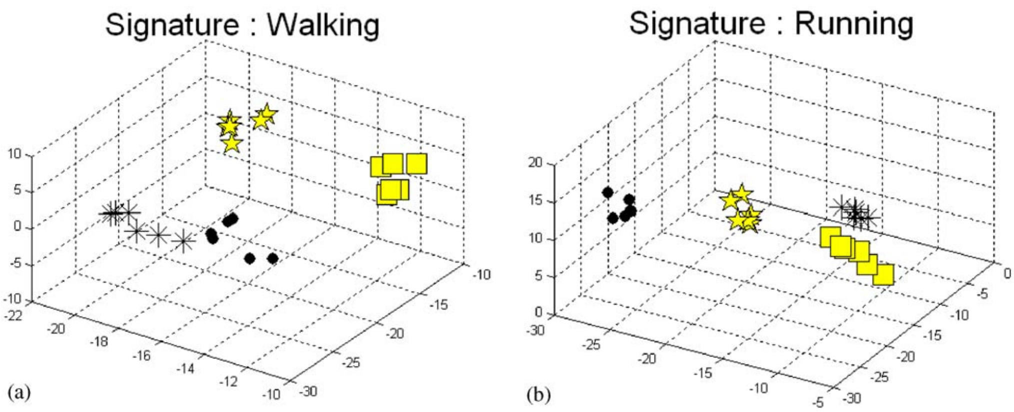

Fig. 15. Feature (phase-weighted magnitude) space of 4 walking and running subjects. X: 1st component of θ_T; Y: 2nd component of θ_T; Z: 1st component of θ_K.

(sample) variance for the PWM signature in Table 1. This is reflected in the recognition rates for walking and running, Fig. 17, which show walking with less discriminatory power than for running. This is confirmed by the ratio of separation to variance which is greater for running, except when higher order components are included in the signature. Conversely, this also implies that walking is more stable. These, amongst other factors, merit further investigation on a larger database. The recognition rate of running is encouraging since running has more variability across the population compared with walking. This variability does suggest that change in running over time could be a performance issue. in application. Moreover, this is consistent with biomechanical analysis: running involves increasing muscle activities and force [29]; and there exist different manners in which the foot contacts the ground [30]. The features appear to have an individual mapping between the feature space of walking and running on an individual class basis. This may suggest that a mapping might exist that could make the signatures invariant. Further, the recognition rates in Fig. 17 show the forced coupled oscillators model giving consistently improved rates over use of the bilateral symmetric model.

Classification is done via the k-nearest neighbour (k-nn) where $k = 1$ and 3, with cross validation and the leave one out rule. No doubt a more sophisticated classifier would be prudent, but the interest here is to examine the genuine discriminatory ability of these features. This technique has been evaluated on clean images of resolution 130×190, see Fig. 16(a). Performance analysis in Fig. 16(b) 25% grey scale noise and (c) low resolution (50% of the original resolution), has also been evaluated. The results from the forced coupled oscillator model in Fig. 17 are included in Fig. 18 for comparison. As expected, the recognition rate decreased when grey scale noise was added. The rate decreased less when the technique was evaluated on lower resolution im-

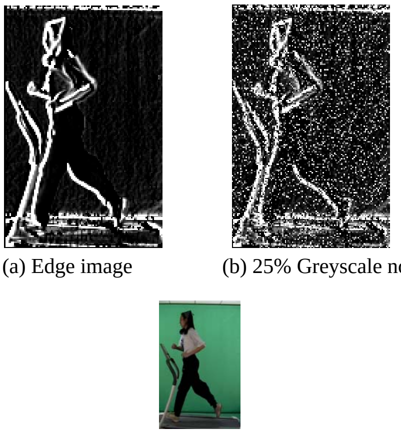

(a) Edge image (b) 25% Greyscale noise

(b) Low resolution (65 x 95)

Fig. 16. Images used for performance analyses.

ages. That the rate does not decrease as much as when tested with noise could be due to measurement of angle of leg rotation is invariant to scaling. It should be noted though that, by appearance, the noise in Fig. 16(b) is similar to that of very poor quality video.

Finally, we sought to determine the effect of the combined leg model, as opposed to the use of just the thigh. Fig. 19 shows the results via single models and the combined model. This shows that modelling both major parts of the leg has indeed improved recognition performance. These results also show greater discriminatory capability for running as opposed to walking and a recognition rate exceeding 90% confirms the capability of this new approach. Naturally, these results suggest that refinement can be made, but they also confirm that model-based analysis can be deployed to good effect in recognition by gait.

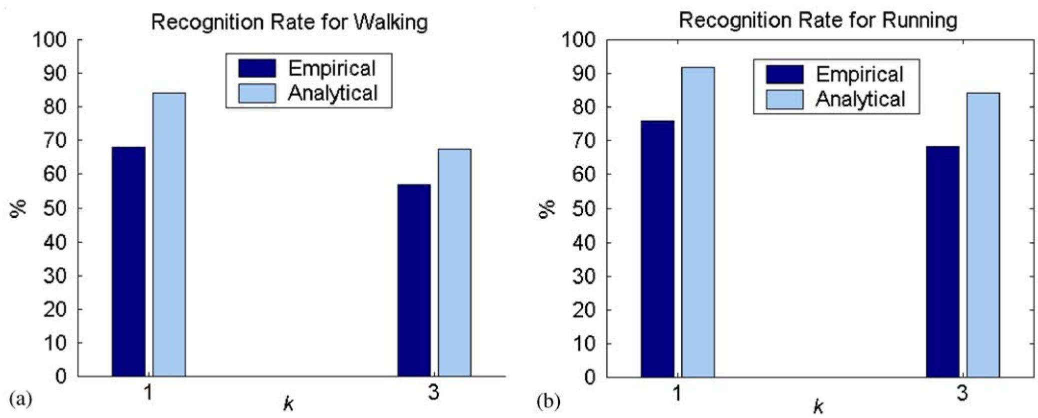

Fig. 17. Recognition rates for walking and running via k-nn with Euclidean distance metric for the bilateral symmetric(empirical) and forced coupled oscillator (analytical) motion model.

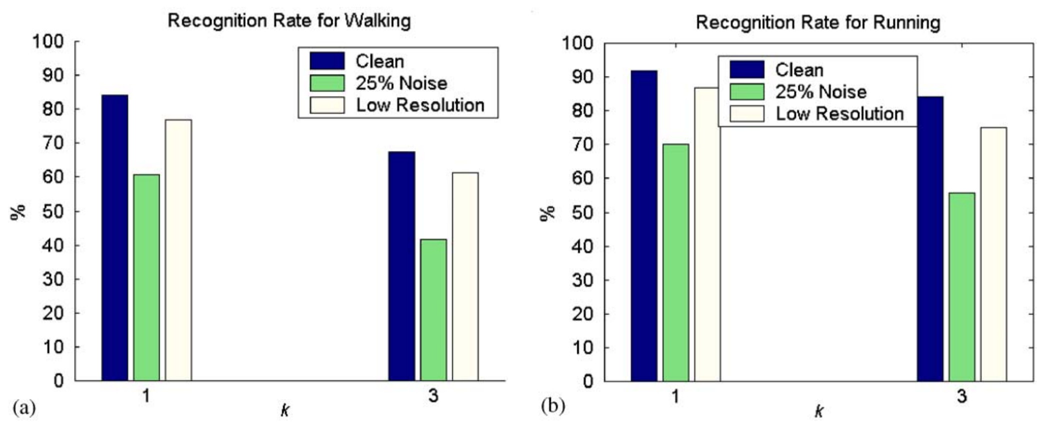

Fig. 18. Performance analysis of walking and running.

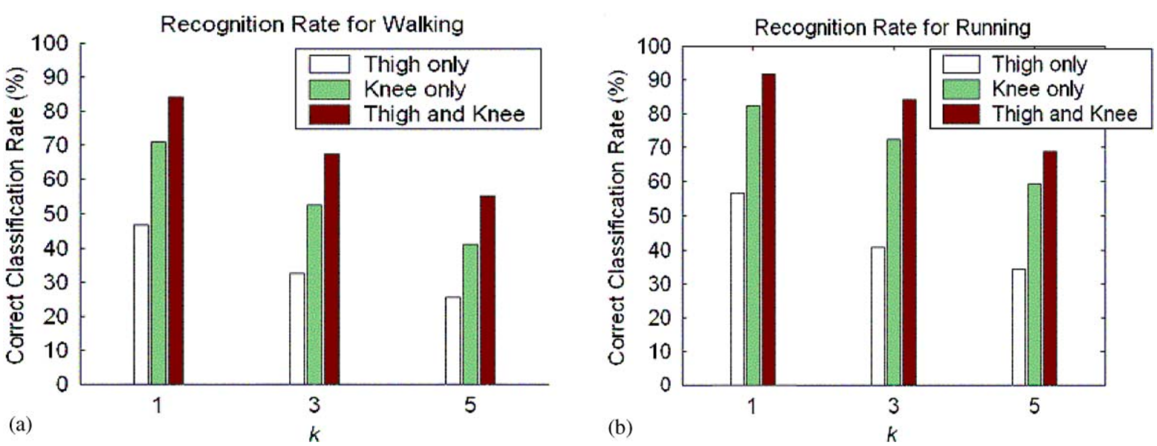

Fig. 19. Comparing the performance of using only the thigh, the knee and both rotations in creating gait signatures.

7. Conclusions and future work

An automated non-invasive system, which can recognise people by the way they walk and by the way they run has been developed. By using pendular motion and the understanding of the biomechanics of human locomotion, two new models, a bilateral symmetric and an analytical model (employing the concept of a forced coupled oscillator) have successfully guided the motion extraction process. Frequency domain gait signatures derived from the motion signals are used for classification. Both models lead to encouraging recognition rates, with the forced coupled oscillator model giving more promising results. This technique has also been evaluated on images with noise and low resolution. Recognition here was affected more by noise then low resolution. This could be due to measurement of angle being invariant to scaling. Analysis shows that both gaits could be potential biometrics. A better recognition rate suggests that running may be more potent compared with walking gait as it has more variation in the gait pattern. This model-based approach may be also useful in fitting noisy or incomplete data in other applications such as tracking and motion recovery, or to guide this process. It may also be deployed for clinical use to offer non-invasive and markerless leg motion extraction [39]. Future work intends to investigate the feature set selection to further increase the recognition rate and also to further improve the forced coupled oscillator model. Since walking and running are intimately related to each other and also given the existence of the individual mapping in the feature space, we aim to determine the nature of the mapping and whether it can be modelled to achieve invariance in gait signature. As the system is described geometrically, camera view angle invariance [40] will be investigated to cope with application issues.

Acknowledgements

We gratefully acknowledge partial support by the European Research Office of the U.S. Army under contract no. N68171-01-C-9002.

References

[1] A.K. Jain, et al. (Eds.), Biometrics—Personal Identification in Networked Society, Kluwer Academic Publishers, Dordrecht, 1999.
[2] L.T. Kozlowski, J.E. Cutting, Recognizing the sex of a walker from a dynamic point-light display, Percep. Psychophy. 21 (6) (1977) 575–580.
[3] G. Mather, L. Murdoch, Gender discrimination in biological motion displays based on dynamic cues, Proc. R. Soc. 258 (1994) 273–279.
[4] J.W. Davis, Visual categorization of children and adult walking styles, Third Proceedings of Audio- and Video-Based Biometric Person Authentication, Halmstaadt, Sweden, 2001, pp. 295–300.
[5] J.E. Cutting, L.T. Kozlowski, Recognizing friends by their walk: gait perception without familiarity cues, Bull. Psychon. Soc. 9 (5) (1977) 353–356.
[6] S. Stevenage, M. Nixon, K. Vince, Visual analysis of gait as a cue to identity, Appl. Cognitive Psychol. 13 (1999) 513–526.
[7] L. Bianchi, D. Angelini, F. Lacquaniti, Individual characteristics of human walking mechanics, Pflugers. Arch - Eur. J. Physiol. 436 (1998) 343–356.
[8] K. Akita, Sequence analysis of real world human motion, Pattern Recognition 17 (1) (1984) 73–83.
[9] Z. Chen, H.J. Lee, Knowledge-guided visual perception of 3D human gait from a single image sequence, IEEE Trans. Syst. Man Cybern. 22 (2) (1992) 336–342.
[10] P. Polana, R. Nelson, Low level recognition of human motion (or how to get your man without finding his body parts), IEEE Proceedings of Computer Society Workshop on Motion of Non-Rigid and Articulated Objects, Austin, Texas, 1994, pp. 77–82.
[11] Q. Cai, J.K. Aggarwal, Tracking human motion using multiple cameras, Proceedings of the International Conference on Pattern Recognition, Vienna, Austria, 1996, pp. 68–72.
[12] J.E. Boyd, J.J. Little, Global versus structured interpretation of motion: moving light display, IEEE Proceedings of the Computer Society Workshop on Motion of Non-Rigid and Articulated Objects, Puerto Rico, 1997, pp. 18–25.
[13] L.W. Campbell, A.F. Bobick, Recognition of human body motion using phase space constraints, Fifth Proceedings of the International Conference on Computer Vision, Cambridge, Massachusetts, 1995, pp. 624–630.
[14] S.A. Niyogi, E.H. Adelson, Analyzing and recognizing walking figures in XYT, Proceedings of the Conference of Computer Vision and Pattern Recognition, Seattle, WA, 1994, pp. 469–474.
[15] H. Murase, R. Sakai, Moving object recognition in eigenspace representation: gait analysis and lip reading, Pattern Recognition Lett. 17 (1996) 155–162.
[16] J. Little, J. Boyd, Recognising people by their gait: the shape of motion, Videre, Int. J. Comput. Vision 14 (6) (1998) 83–105.
[17] P.S. Huang, C.J. Harris, M.S. Nixon, Human gait recognition in canonical space using temporal template, IEE Proc. Vision, Image Signal Process. 146 (2) (1999) 93–100.
[18] C.B. Abdelkader, R. Cutler, H. Nanda, L. Davis, EigenGait: motion-based recognition using image self-similarity, Third Proceedings of the Audio- and Video-Based Biometric Person Authentication, Halmstaadt, Sweden, 2001, pp. 289–294.
[19] J. Foster, M. Nixon, A. Prugel-Bennett, New area based metrics for automatic gait recognition, Proceedings of the British Machine Vision Conference, Manchester, UK, 2001, pp. 233–242.
[20] A.Y. Johnson, A.F. Bobick, A multi-view method for gait recognition using static body parameters, Third Proceedings of the Audio- and Video-Based Biometric Person Authentication, Halmstaadt, Sweden, 2001, pp. 301–311.
[21] J.D. Shutler, M.S. Nixon, C.J. Harris, Statistical gait recognition via temporal moments, Fourth IEEE Southwest Symposium on Image Analysis and Interpretation, Austin, Texas, 2000, pp. 291–295.
[22] J. Hayfron-Acquah, M. Nixon, J. Carter, Recognising human and animal movement by symmetry, IEEE Proceedings of the International Conference on Image Processing, Thessaloniki, Greece, 2001, pp. 290–293.

[23] D. Cunado, M.S. Nixon, J.N. Carter, Gait extraction and description by evidence-gathering, Comput. Vision Image Understanding 90 (1) (2003) 1–41.
[24] V.M. Zatsiorky, S.L. Werner, M.A. Kaimin, Basic kinematics of walking: step length and step frequency: a review, J. Sports Med. Phys. Fitness 34 (2) (1994) 109–134.
[25] L. Li, E.C.H.v.d. Bogert, G.E. Caldwell, R.E.A.v. Emmerik, J. Hamill, Coordination patterns of walking and running at similar speed and stride frequency, Hum. Movement Sci. 18 (1999) 67–85.
[26] Aristotle, On the Gait of Animals, Part 7 (384–322 B.C.).
[27] M. Murray, Gait as a total pattern of movement, Am. J. Phys. Med. 46 (1) (1967) 290–332.
[28] P.R. Cavanagh, Biomechanics of Distance Running, Champaign, IL: Human Kinetics Books, 1990.
[29] S. Ounpuu, The biomechanics of walking and running, Clin. Sports Med. 13 (4) (1994) 843–863.
[30] D.B. Thordarson, Running biomechanics, Clin. Sports Med. 16 (2) (1997) 239–247.
[31] I. Stewart, Symmetry-breaking cascades and the dynamics of morphogenesis and behaviour, Sci. Prog. 82 (1) (1999) 9–48.
[32] H. Sadeghi, P. Allard, F. Prince, H. Labelle, Symmetry and limb dominance in able bodied gait: a review, Gait Posture 12 (2000) 34–45.
[33] G.J.V.I. Schenau, Some fundamental aspects of the biomechanics of over ground versus treadmill locomotion, Med. Sci. Sports Exercise 12 (1980) 257–261.
[34] M.P. Murray, G.B. Spurr, S.B. Sepic, G.M. Gardner, Treadmill vs. floor walking: kinematics, electromyogram, and heart rate, J. Appl. Physiol. 59 (1985) 87–91.
[35] J.C. Wall, J. Charteris, The process of habituation to treadmill walking at a different velocities, Ergonomics 23 (1980) 425–435.
[36] D. Cunado, M.S. Nixon, J.N. Carter, Automatic gait recognition via model-based evidence gathering, IEEE Proceedings of the Workshop on Automated ID Technologies Summit, NY, 1999, pp. 27–30.
[37] K.G. Holt, The force-driven harmonic oscillator as a model for human locomotion, Hum. Movement Sci. 9 (1990) 55–68.
[38] C. Angeloni, P.O. Riley, E.D. Krebs, Frequency content of whole body gait kinematic data, IEEE Trans. Rehabilitation Eng. 2 (1) (1994) 40–46.
[39] C.-Y. Yam, M.S. Nixon, J.N. Carter, Automated markerless analysis of human walking and running by computer vision, Proceedings of the World Congress of Biomechanics, Calgary, Alberta, 2002.
[40] J. Carter, M. Nixon, On measuring gait signatures which are invariant to their trajectory, Meas. Control 32 (1999) 265–269.

About the Author—CHEW-YEAN YAM received her B. Eng. (1999) in Computer Engineering and Ph.D. (2003) in Computer Vision from the Department of Electronics and Computer Science, University of Southampton, UK. Her research interest includes computer vision, pattern recognition, human motion understanding and analysis, and biometrics.

About the Author—MARK S. NIXON is the Professor of Computer Vision in the Image Speech and Intelligent Systems Research Group, University of Southampton where he leads the vision research team. His team was one of the early pioneers of gait as a biometric, with research currently funded under DARPA's Human ID at a Distance programme. His other interests include in particular developing new techniques for feature extraction and description, especially moving ones, with applications in medical imaging, biometrics and remote sensing. His new textbook *Feature Extraction and Image Processing*, co-authored with Alberto S. Aguado, was published by Butterworth Heinemann in 2002. As well as other meetings, he has co-chaired the *British Machine Vision Conference BMVC 98* (Southampton 1998) and the *Fourth Audio Visual Biometric Person Authentication AVBPA 2003* (Guildford 2003) and is Proceedings Chair for the forthcoming *ICPR 2004* at Cambridge.

About the Author—JOHN N. CARTER graduated first in Physics from University College, Dublin and later with a PhD in Astrophysics from the University of Southampton. Currently, he is a Senior Lecturer in the Image Speech and Intelligent Systems Research Group, University of Southampton. He is co PI on Southampton's part of the DARPA Human ID at a Distance programme. Currently he is working in the general area of Four-Dimensional Image Processing. That is, analysing sequences of images to extract both two and three dimensional features, exploiting coherence over the whole sequence. Measuring the shape of the human vocal tract is another long term interest. Recent successes in developing a new form of Dynamic Magnetic Resonance Imaging has made it possible to reconstruct signal and multi-planar views of the vocal tract while a subject is saying a short repetitive speech cycle.